

***In Situ* Observations on Effects of Hydrogen on Deformation and Fracture of A533B Pressure Vessel Steel**

H.E. Hänninen, T.C. Lee, I.M. Robertson, and H.K. Birnbaum

External hydrogen gas atmospheres enhanced dislocation motion, multiplication of dislocations, and dislocation source activation under applied loading during *in situ* high-voltage electron microscopy (HVEM) observations of A533B pressure vessel steel. However, in both vacuum and hydrogen atmospheres, fracture occurred in a ductile manner in specimen areas transparent in the 1000-keV HVEM. The principal effect of the hydrogen atmosphere was to decrease the stress required for deformation near the crack tip and for crack propagation. Deformation at the crack tip was highly localized in both atmospheres, and a yielding strip plastic zone, analogous to the Dugdale-Barenblatt model for crack growth, formed ahead of the crack tip. The crack tip plasticity was confined to this strip. Inside the yielding strip, final cracking occurred through a sliding-off mechanism in the thin areas of the HVEM specimen. In the thicker areas of the specimen, where the yielding strip ahead of the crack was no longer transparent, crack tip blunting and void/microcrack formation ahead of the main crack tip could be observed directly. Crack tip blunting occurred by a two-corner mechanism, and further crack growth initiated by strain localization at one of the crack tip vertices. Also void/microcrack formation ahead of the main crack tip was operative and resulted in coalescence into the main crack tip along the anticipated shear bands. Fractography of the thicker areas showed a ductile, dimpled fracture mechanism both in vacuum and hydrogen atmospheres.

Keywords

crack tip mechanisms, fracture, hydrogen embrittlement, pressure vessel steel

1. Introduction

RECENT observations have shown that most types of hydrogen-induced fracture modes are at least microscopically ductile even though macroscopically brittle behavior is observed. As a result, it has been proposed that hydrogen-enhanced plasticity and strain localization, which are directly associated with the hydrogen-induced fracture, are the controlling factors in hydrogen-induced cracking of iron and steels.^[1-3] Direct, *in situ* high-voltage electron microscopy (HVEM) studies of iron under constant applied deflection have revealed that external hydrogen gas enhanced dislocation motion, multiplication of dislocations, and dislocation source activation when compared to the behavior in vacuum.^[4,5] In these experiments, the hydrogen concentrations were not determined, but the hydrogen fugacity has been shown to be relatively high because of electron beam dissociation and ionization of the hydrogen molecules.^[6] The mechanism of hydrogen-induced reduction of the flow stress (softening) in iron is a complex phenomenon, and it can take place by enhancing the motion and multiplication of dislocations either by reducing the friction stress due to weak-

ening of the strength of the interatomic bonds,^[7] or by shielding the dislocation interactions with other dislocations, solute atoms, or precipitates.^[8]

In hydrogen charging studies, contradictory experimental results, either softening or hardening, have been observed depending on the charging conditions (hydrogen fugacity, temperature, strain rate, purity of iron, and other significant experimental factors).^[9] In general, there seems to be some disagreement with the observations obtained in thin-foil HVEM specimens (plane-stress conditions) and the material behavior in the thicker sections (plane-strain conditions), where hydrogen-induced softening is observed in very limited conditions. In notched bulk specimens, however, hydrogen-charged steel specimens have shown localized shear banding along characteristic slip traces, under conditions where uniform plastic flow occurred in the uncharged specimens.^[10,11] These shear bands promoted void nucleation and growth at carbide/matrix interfaces, thus enhancing fracture. Consequently, the main interest is how well the HVEM observations can explain the effects of hydrogen on the deformation processes ahead of the crack tip in the bulk specimens, where the deformation processes are different from the smooth tensile specimens and are highly localized.

Crack growth in thin HVEM specimens can be examined through a simple model for fully developed plane-stress yielding in thin sheets, where no strain constraints and stress elevation exist, such as the Dugdale-Barenblatt model.^[12,13] In this model, yielding is assumed to be confined to a narrow zone directly ahead of the crack tip, and yielding is considered to make the crack longer by an amount equal to the plastic zone size ahead of the crack tip. The cohesive stresses inside the plastic zone (on the extended fracture surface) act to restrain the crack opening. The restraining stress is either the constant yield

H.E. Hänninen, Technical Research Centre of Finland, Metals Laboratory, SF-02150 Espoo, Finland; presently at Helsinki University of Technology, Laboratory of Engineering Materials, SF-02150 Espoo, Finland; and **T.C. Lee**, **I.M. Robertson**, and **H.K. Birnbaum**, Materials Research Laboratory, University of Illinois, Urbana, IL 61801, USA.

Table 1 Chemical composition of A533B pressure vessel steel

C	Mn	P	S	Composition, wt%		Cr	Mo	V	Cu
				Si	Ni				
0.19	1.28	0.009	0.013	0.25	0.61	0.04	0.55	0.004	0.10

stress, σ_y , in the case of small-scale yielding and perfect plasticity, or the flow stress in the case of strain hardening. The crack tip opening, δ_p , is a measure of deformation (stretching) occurring in the crack tip plastic zone. The narrow region where yielding is localized has a height roughly equal to the sheet thickness, h , and therefore, the average plastic strain, ϵ_p , in the crack growth is approximately:^[14,15]

$$\epsilon_p = \delta_t / h \quad [1]$$

The crack tip opening, δ_p , has been solved for the case of perfect plasticity and constant cohesive stress, σ_y :^[16]

$$\delta_t = K^2/E \cdot \sigma_y \quad [2]$$

The corresponding plastic zone size is then

$$r_p = \pi/8 \cdot K^2/\sigma_y^2 \quad [3]$$

Physically, the Dugdale-Barenblatt model can be interpreted by through-the-thickness slip and necking. It has been found that the crack tip opening displacement (CTOD) is equal to the thickness reduction within the strip yielding zone. This thickness reduction, Δh , is therefore also related to the applied K value at fracture according to the Dugdale-Barenblatt model for small-scale yielding.^[15]

$$\Delta h = \text{CTOD} = K^2/E \cdot \sigma_y \quad [4]$$

Thus, K values at the crack tip can also be calculated for stable crack growth by sheet thickness reduction measurements along the crack path. The specimen size requirements for valid K_{Ic} test procedures are, however, not satisfied; for valid J_{Ic} test results, the specimen thickness should be in this case about 1 mm ($K_c = 20 \text{ MPa}\sqrt{\text{m}}$, $\sigma_y = 500 \text{ MPa}$).

In the present study, the effects of hydrogen on A533B pressure vessel steel deformation, crack tip blunting, microvoid/crack formation ahead of the crack tip, and fracture properties have been studied by using the *in situ* deformation technique in the environmental cell of a HVEM as used before by Tabata and Birnbaum^[4,5] for iron.

2. Experimental Procedure

The test material, A533B steel, was taken from a 1CT-corrosion fatigue test specimen used in the international cyclic crack growth rate round robin test using test specimens provided by Electric Power Research Institute (EPRI).^[17,18] The chemical composition of the A533B steel is shown in Table 1. HVEM specimens were made by rolling to a thickness of 50 μm . These

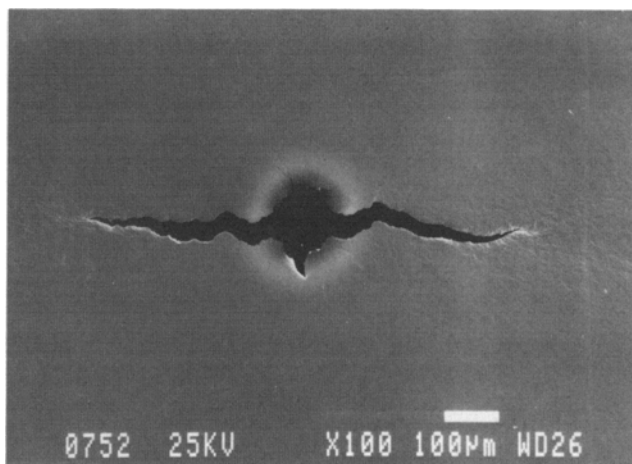
foils were then heat treated in a manner similar to the original bulk material (austenitized at 1172 K for 20 h, water quenched, tempered at 944 K followed by air cooling and subsequently stress relieving at 839 K for 5 h and at 894 K for 125 h). The original material had a tempered bainite microstructure, consisting of bainite laths, which were subdivided by a dislocation wall structure and which contained carbides of the types of M_3C , M_{23}C_6 , and Mo_2C .^[18] Annealed thin-foil specimens were finally thinned by chemical etching in a solution of HF and H_2O_2 (1:20), followed by jet polishing using a solution of perchloric acid and acetic acid (1:10) at room temperature until a hole formed in the middle of the tensile specimen. Areas around the hole were sufficiently thin for electron transmission.

In situ observations of plastic deformation and fracture were carried out in the Argonne National Laboratory HVEM environmental test cell. The tensile stage used operated under displacement control and was driven by an electric motor. Specimens were first loaded in vacuum (10^{-3} Pa). When the initial crack formed, the plastic deformation ahead of the crack tip and the fracture processes were studied by adding and removing low partial pressures of hydrogen gas (up to 300 torr) to the environmental cell at room temperature. The hydrogen fugacity in the cell with the electron beam present is significantly greater because of dissociation and/or ionization of molecular H_2 .^[6] At higher hydrogen pressures, electron scattering from the gaseous atmosphere markedly reduced the contrast of the electron image.

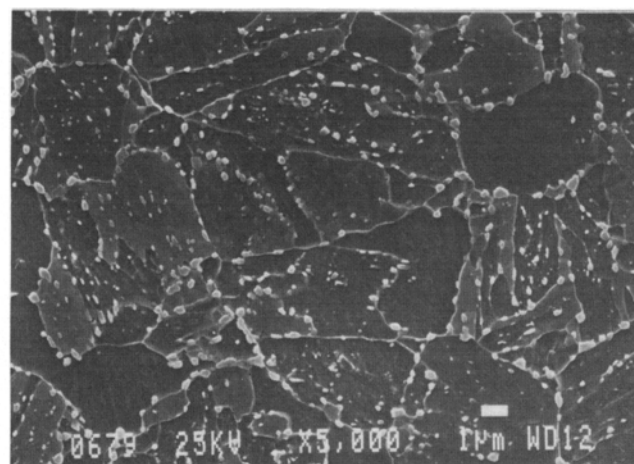
Cracks initiated from the center hole and propagated into thicker sections of the specimen (Fig. 1a). During observations of hydrogen effects on plastic deformation occurring at the crack tips under stress, displacement was generally held constant. When the total specimen displacement was constant, the stress in the specimen stayed constant, if no additional plastic deformation occurred, or decreased if it plastically relaxed. The test facility did not allow constant-load crack growth tests. It was possible to increase the stress by increasing the displacement and was also possible to perform constant-displacement rate tests *in situ*. The deformation and fracture phenomena were recorded on videotape, from which image processing was used to form individual images.

3. Experimental Results and Discussion

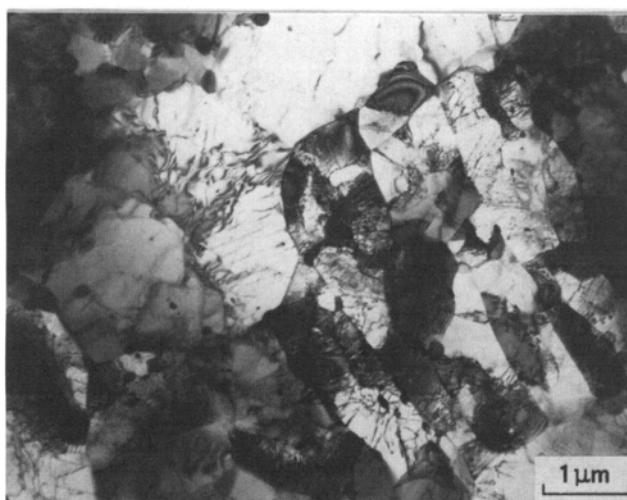
The microstructure of the A533B steel is shown in Fig. 1(b) and (c). It is similar to the original microstructure of bulk specimens, but the grain size is somewhat smaller, about 10 μm . Direct *in situ* observations in the HVEM of A533B pressure vessel steel confirmed the earlier observations of Tabata and Birnbaum^[4,5] of hydrogen effects on dislocation generation and motion as well as fracture in iron. Introduction of hydrogen gas into the environmental chamber above a certain pressure enhanced dislocation motion and multiplication in the speci-



(a)



(b)



(c)

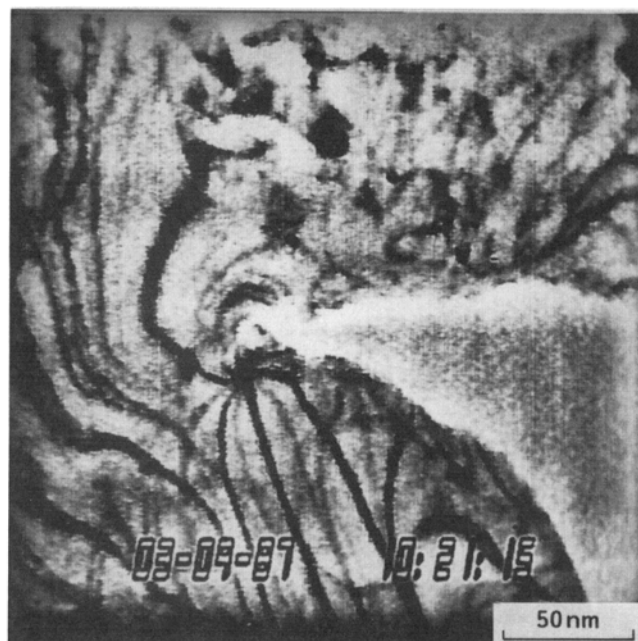
Fig. 1 (a) General view of a crack initiating from the center hole of the HVEM specimen. (b) and (c) Microstructure of the A533B pressure vessel steel.

mens held under constant deflection, under which no dislocation activity was observed in vacuum. In addition, dislocations in cell walls were released, and they became mobile dislocations on the addition of hydrogen gas. Thus, hydrogen appeared to increase the rate of microstructural changes under stress. The dislocation activity was dependent on hydrogen gas pressure and stress, i.e., crack tip stress intensity, when areas ahead of the cracks were examined. Under constant hydrogen pressure and displacement, deformation relaxed the stresses, and the dislocation activity slowly decreased. When hydrogen gas was removed from the environmental chamber, the dislocation activity stopped immediately, and when hydrogen gas was reintroduced into the environmental chamber, the dislocation activity started just above the gas pressure value that was previously applied. Thus the dislocation activity ahead of the loaded crack tip was dependent both on the load and hydrogen fugacity in a reproducible manner, indicating that the critical

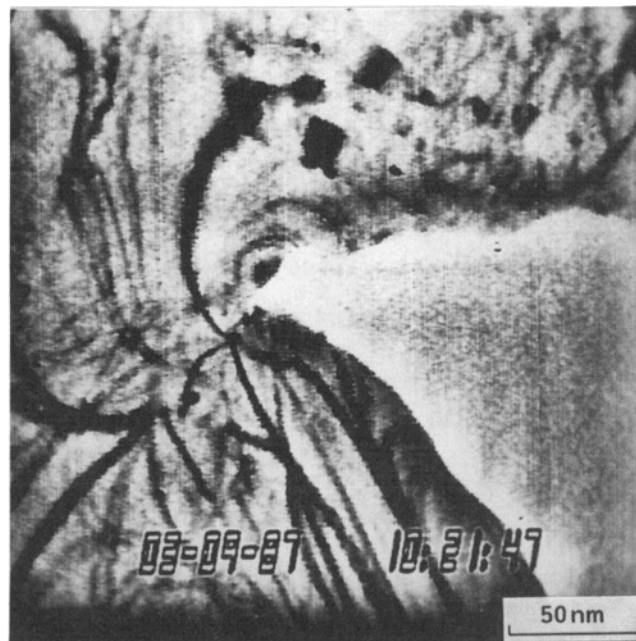
stress-intensity value for crack growth is directly dependent on hydrogen fugacity.

The basic fracture mechanisms in vacuum and in hydrogen gas seemed to be ductile rupture in both cases. The difference in fracture between vacuum and hydrogen environments was that the load required to induce plasticity ahead of the crack tip was reduced by hydrogen. In the microstructure studied, no hydrogen-induced localization of deformation was observed. In both cases, the deformation was localized in the yielding strip plastic zone formed ahead of the crack tip. The observed fracture mode in both atmospheres was always transgranular, ductile fracture. No brittle, rapid crack growth was observed.

In the thin sections of the specimens, crack formation took place by a sliding-off mechanism along slip planes of the steel (Fig. 2). When the crack grew from the thin middle section of the specimen into the thicker areas, plastic thinning took place at the crack tip, and the dislocation activity occurred ahead of



(a)



(b)

Fig. 2 Cracking in thin section of HVEM specimen in hydrogen atmosphere taking place by a sliding-off mechanism.

the crack tip in the yielding strip. Figure 3 shows successive deformation stages in a thinned area ahead of a crack tip taken from the videotapes of the complete fracture process. Inside the yielding strip, the dislocation motion and multiplication was dependent on the loading and hydrogen fugacity in the manner summarized above. Small carbide particles acted as dislocation sources ahead of the crack tip inside the yielding strip. Almost dislocation-free zones were observed around the small particles (see particle A in Fig. 3b) acting as dislocation sources.

Ohr^[19] suggested that a dislocation-free zone formed between the crack tip and the plastic zone further ahead of the crack tip. However, in the pressure vessel steel specimens studied, the crack tip did not propagate by emission of dislocations into the material from the crack tip. Dislocation generation occurred ahead of the crack tip from small particles, as well as from cell walls inside the yielding strip, while they were breaking down, and from thick, dense tangled dislocation walls formed on both sides of the yielding strip. In particular, small particles operating as dislocation sources appeared to control the critical strain at which the shear band formation (flow localization) took place. The dislocations generated ahead of the crack tip inside the yielding strip formed thick, dense tangled dislocation walls on both sides of the yielding strip plastic zone (Fig. 4a). Dislocations were also observed to move from interior sources into the crack tip. The thick, dense tangled dislocation walls are left behind the crack tip in the wake of the crack, after fracture has taken place, as residual plastic zones.

Plasticity is confined to the yielding strip ahead of the crack tip. This yielding strip is a manifestation of the Dugdale-Barenblatt model for fracture under plane-stress state loading. The Dugdale-Barenblatt yielding strip model has been analyzed by introducing a continuous dislocation distribution ahead of the crack tip to account for the plastic zone.^[20] Based on this as-

sumption, an infinite dislocation density at the immediate crack tip could be expected. The present direct *in situ* observations, however, reveal the opposite, because apparently a very low dislocation density exists just ahead of the crack tip inside the yielding strip under sustained loading. The yielding strip is thus softer than its surroundings, which confines the plastic deformation into this soft region of lower dislocation density. This yielding strip is analogous to shear bands, which are known to form in the heavily deformed metals, when the more homogeneous deformation mechanisms break down.^[21] In fatigue, flow localization is manifested in the form of persistent slip bands (PSB).^[22] Based on these observations, the main role of hydrogen is to enhance dislocation emission and motion inside the crack tip yielding strip by softening the material locally ahead of the crack tip.

The relationship between this kind of yielding strip/shear band, typical for plane stress, and the plasticity in front of a blunted crack tip in a bulk specimen is not established. In particular, whether this kind of yielding strip/shear band is formed as a part of the process zone formed ahead of the crack tip under the plane-strain stress state is not known. In this situation, the yielding strip (shear band) formation would change the crack tip strain field markedly ahead of the blunted crack tips, and the strain intensification required for crack growth would be readily attained within the yielding strip where the flow is localized. This would then result in premature loss of load-bearing capacity at the crack tip. The role of hydrogen would be understood through its effects on local enhancement of plastic deformation by enhancing dislocation motion, multiplication of dislocations, and dislocation source activation, as well as increasing the dislocation density in dislocation tangles compared to the behavior in inert environments.

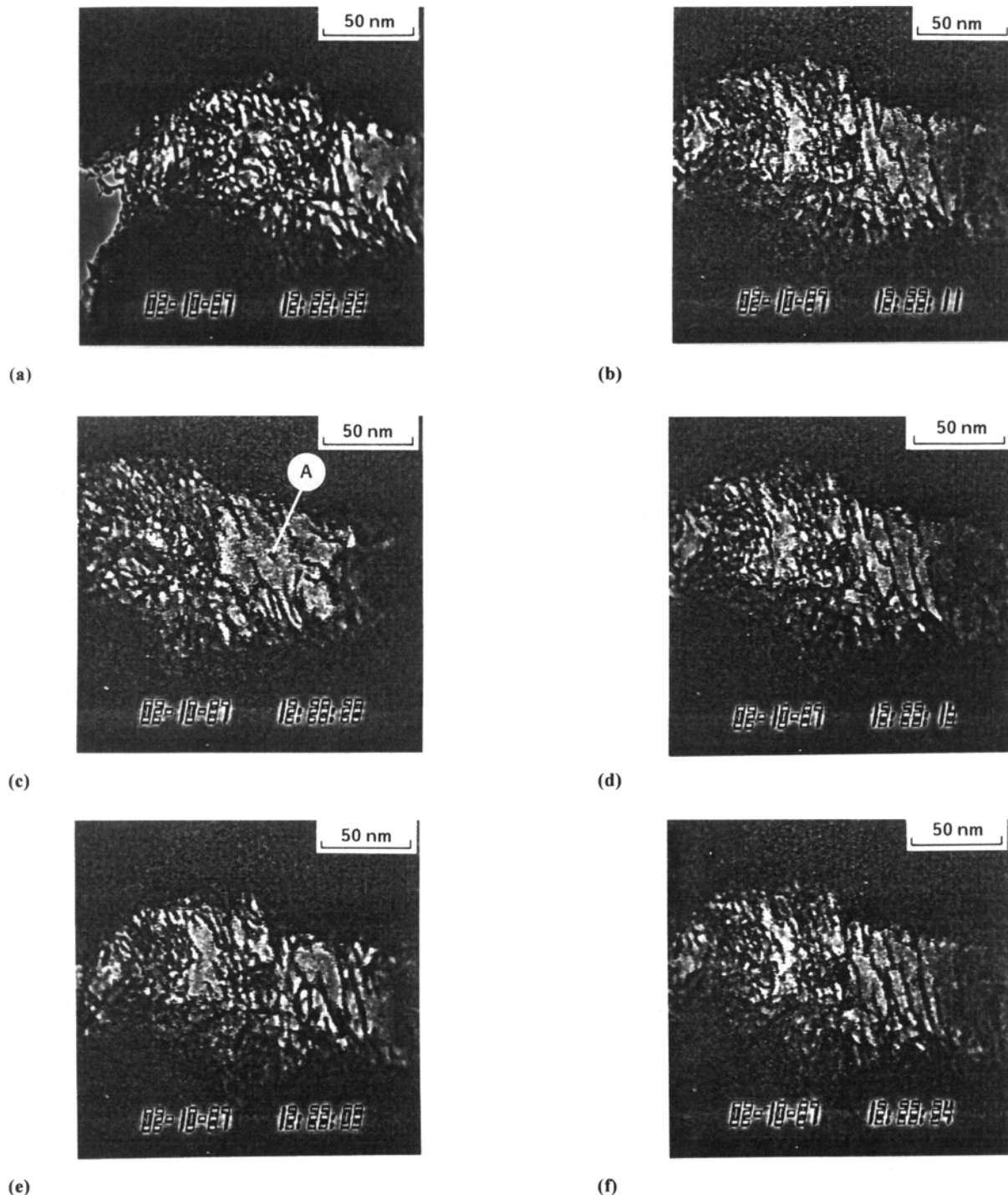
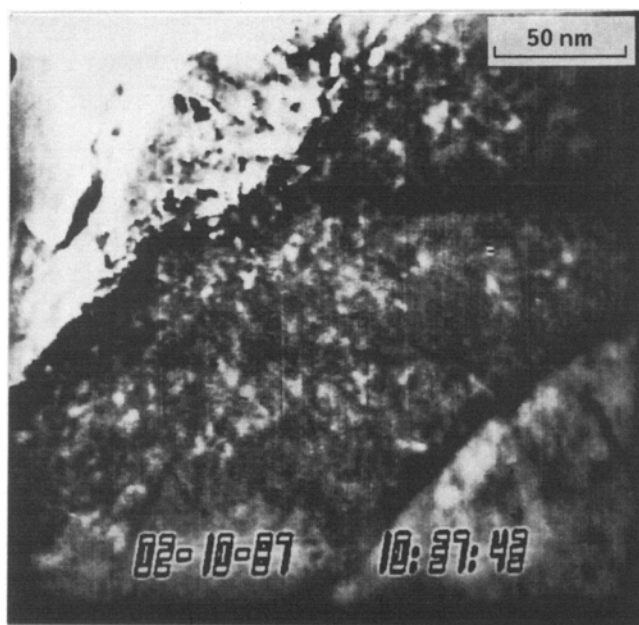


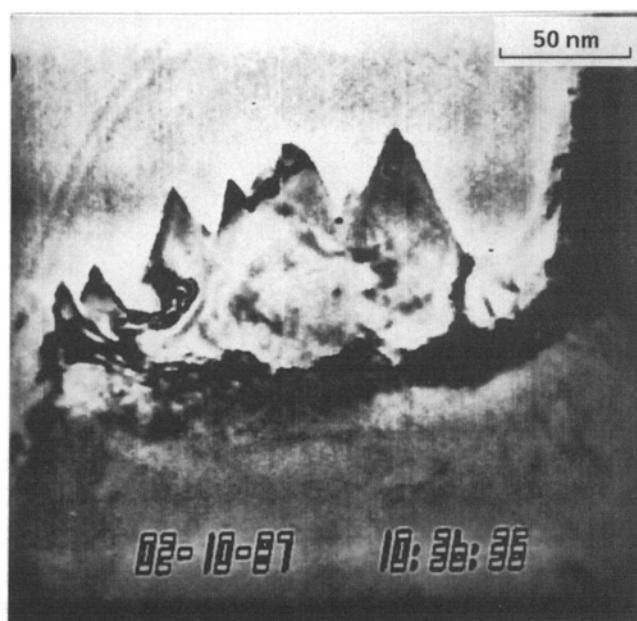
Fig. 3 Successive stages of plastic deformation in hydrogen atmosphere ahead of the crack tip in the yielding strip. Note that the dislocation activity is taking place inside the yielding strip and dislocations are stuck into the thick, dense, tangled dislocation walls formed on both sides of the yielding strip. (Exact times are noted in the figures.)

In the final stage, the crack grows through the thinned region forming a zig-zag pattern (sliding-off type of fracture inside the yielding strip), as shown in Fig. 4(b). The profile likely consists of slip planes, which is consistent with the concept of ductile fracture mechanisms.^[23] In thicker areas, which are no longer transparent in the 1000-keV HVEM, the crack growth

took place primarily by void/microcrack formation ahead of the crack tip and linkage to the main crack tip. Crack tip blunting occurred through a two-corner mechanism, resulting in a flat-nosed crack tip (Fig. 5a). Further loading caused sharpening in one of the crack tip corners (Fig. 5b), and when loading was continued further, microcracks/voids formed ahead of the



(a)



(b)

Fig. 4 (a) Thick, dense, tangled dislocation wall aligned with yielding strip after fracture has occurred. This dislocation wall represents the residual plasticity in the wake of the crack. (b) Fracture surface profile inside the yielding strip showing a zig-zag pattern.

crack tip (Fig. 5c). Another example of void initiation ahead of the main crack tip is presented in Fig. 6, which also shows the linkage of the voids to the main crack tip. From Fig. 5 and 6, it can be seen that the void formation occurs primarily along the curved surfaces, approximately representing the slip-line field ahead of the crack tip process zone. Even though the yielding strip formation observed in thinner areas is not directly observable in thick areas, one can anticipate that dislocation processes, similar to those observed in the thin section, are taking place in the thick section as well. Thus, void/microcrack formation takes place inside the yielding strip, probably at small particles and possibly also at dislocation cell walls, as well as at bainite packet and grain boundaries present in the yielding strip. Linkage between the voids/microcracks and the main crack tip seems to occur along the slip-line traces after formation of shear bands by a sliding-off mechanism through the shear band. In these specimens, the void/microcrack formation ahead of the crack tip took place generally at distances between two to five times the CTOD observed in the HVEM, but there were occasions where voids initiated up to seven times the CTOD ahead of the crack tip (Fig. 6a). Therefore, void initiation is most probably connected with sites of local deformation inside the yielding strip plastic zone. Even though dislocations were not visible in thick sections, enhanced void formation and thinning in hydrogen atmospheres is evidence for increased plasticity compared to vacuum.

Crack tips were studied in the scanning electron microscope (SEM). Figure 1(a) shows the general view of a specimen, exhibiting the center hole from where the cracks were initiated and the thin area around the hole where the HVEM observations were recorded. Detailed views of the crack tip at both ends of a crack are shown in Fig. 7. Thinning ahead of the crack tip

is evident in both crack tips, extending about 50 μm ahead of the main crack tip. In the necked zone ahead of the crack tip, and in the crack wake, the grain boundaries have become visible; the crack changes its orientation while passing the grain boundary (note particularly the crack tip shown in Fig. 7a). Inside the yielding strip ahead of the crack tip (Fig. 7b), sites where voids are forming are visible in front of the crack, as was shown in the HVEM specimens shown in Fig. 5 and 6. Sites A are inside the grain and sites B are very near the grain boundary, probably representing void initiation at small particles and at grain boundaries, respectively.

The SEM study indicates that the flat-nosed type of blunting at the crack tip takes place when the crack tip is dormant at a grain boundary and that the localized deformation at one of the crack tip vertices initiates the penetration across the grain boundary. At the sharp crack tip vertex, a change in the loading path from uniaxial tension to shear takes place easily, resulting in flow localization/shear banding. Further plastic flow is confined into these shear bands rather than exhibiting general yielding. Fracture then proceeds by shear banding/flow localization combined with other processes such as void formation and coalescence inside the shear bands, resulting in the mode of ductile fracture observed in this study. The presence of hydrogen allows these ductile processes to occur at lower stress levels. In addition, it is possible that hydrogen-induced decohesion of grain boundaries, particle/matrix interfaces, and other interfaces can take place.

Crack tip areas exhibit marked thinning extending about 50 μm ahead of the crack tip, marked as point C in Fig. 7(a) and (b). The yielding strip zone is embedded within a more diffuse plastic zone extending about 200 μm ahead of the crack tip. However, exact determination of the size of the diffuse plastic

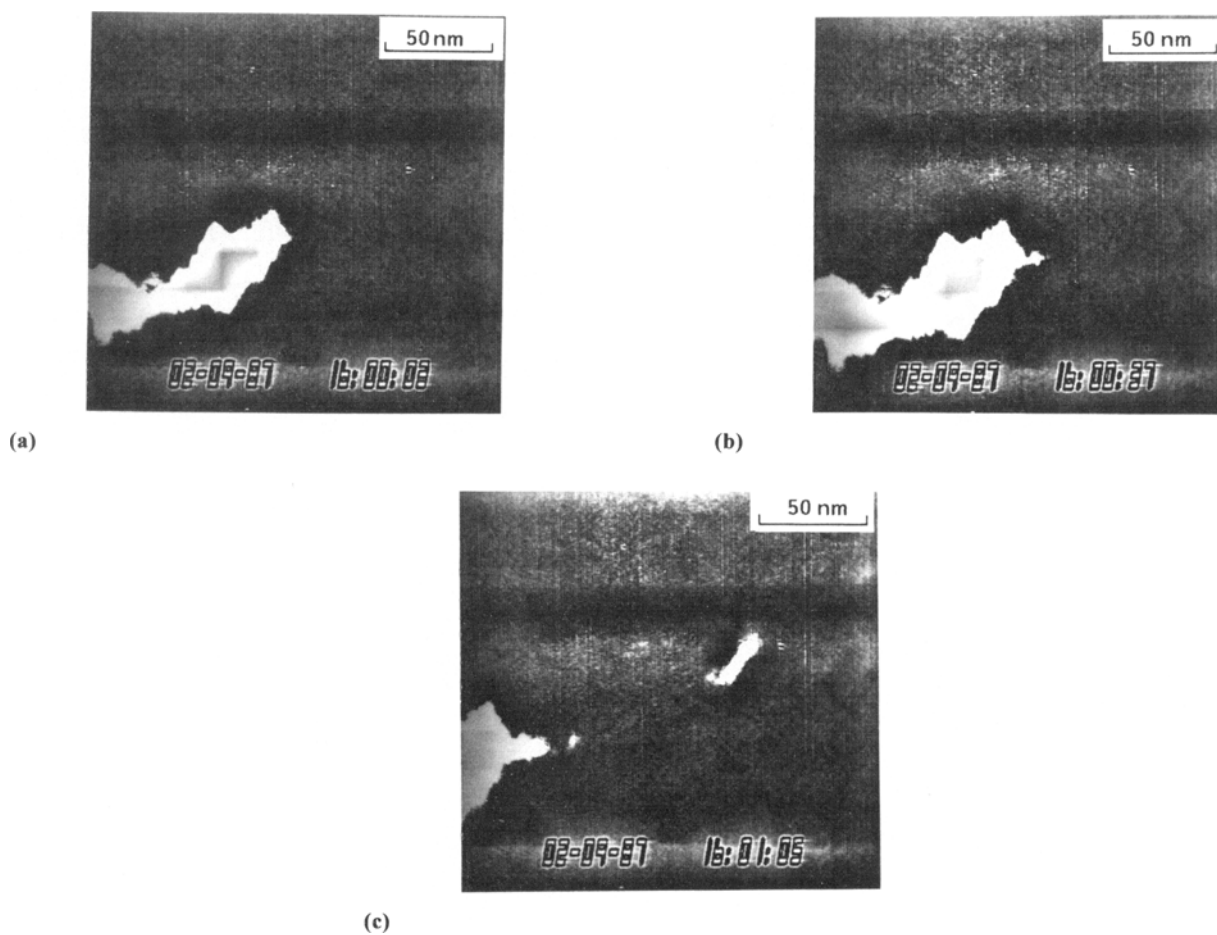


Fig. 5 Successive stages of crack growth under increasing deflection in 200 torr hydrogen atmosphere showing crack tip blunting and sharpening at one of the crack tip corners due to strain localization as well as void/microcrack formation ahead of the crack tip.

zone is very difficult. The distribution of plastic deformation ahead of the crack tip would have been easier to observe if the specimens were etched before HVEM examination so that the grain boundaries and particularly the small particles were more visible.

Figure 8 shows the fractography of one of the cracks formed in the specimen shown in Fig. 1(a) along the crack path with various thicknesses. In thin sections of the specimen, cracking takes place primarily through the sliding-off mechanism (Fig. 8a). When the thickness of the specimen increases, the ductile, dimpled fracture zone in the middle of the specimen becomes evident (Fig. 8b and c). From the fracture surfaces, it is impossible to distinguish between zones cracked in vacuum or in hydrogen; both conditions resulted in similar fracture surfaces. By comparing the fracture profiles in Fig. 7 and the fracture surfaces in Fig. 8, it can be concluded that the ductile, dimpled fracture occurs along the shear bands through a sliding-off mechanism on a small scale. The blunting of the crack tip at grain boundaries and subsequent strain localization and fracture along different directions in the next grain is not discernible from the fracture surface in the thicker sections of the specimens (Fig. 8).

The thickness reduction before fracture did not show any clear indications of possible environmental effects. This is con-

sistent with the authors' observations that the effect of hydrogen is primarily to decrease the stress at which the ductile rupture occurs. It is clear from Fig. 8 that the thickness reduction is largest in the thinnest sections ($\Delta h = 7/8$) and that Δh decreases as the section thickness increases; being about three-fourths of the specimen thickness in Fig. 8(b) and about two-thirds of the specimen thickness in Fig. 8(c). Thus, the average strain accompanying crack growth decreases as the crack penetrates into thicker sections of the specimen. Estimation of crack tip opening displacement from the SEM photographs is very difficult in these specimens. It is reasonable to assume that Δh is equal to the CTOD. If the measured values of Δh are applied in Eq 4 and it is assumed that σ_y is 500 MPa at room temperature and that E is 2×10^5 MPa, K values between 20 to 25 $\text{MPa}\sqrt{\text{m}}$ are obtained for cracking in both hydrogen and vacuum. These are very low values compared to the typical K_{Ic} values obtained at room temperature for A533B pressure vessel steel tested in benign environments. Typical K_{Ic} values for this steel are ten times higher than these values calculated from TEM specimens. However, the lowest measured K values for environment-enhanced cracking (EAC) are on this order, indicating possible consistency between the hydrogen-related phenomena observed in these measurements and in environment-enhanced cracking of this steel.

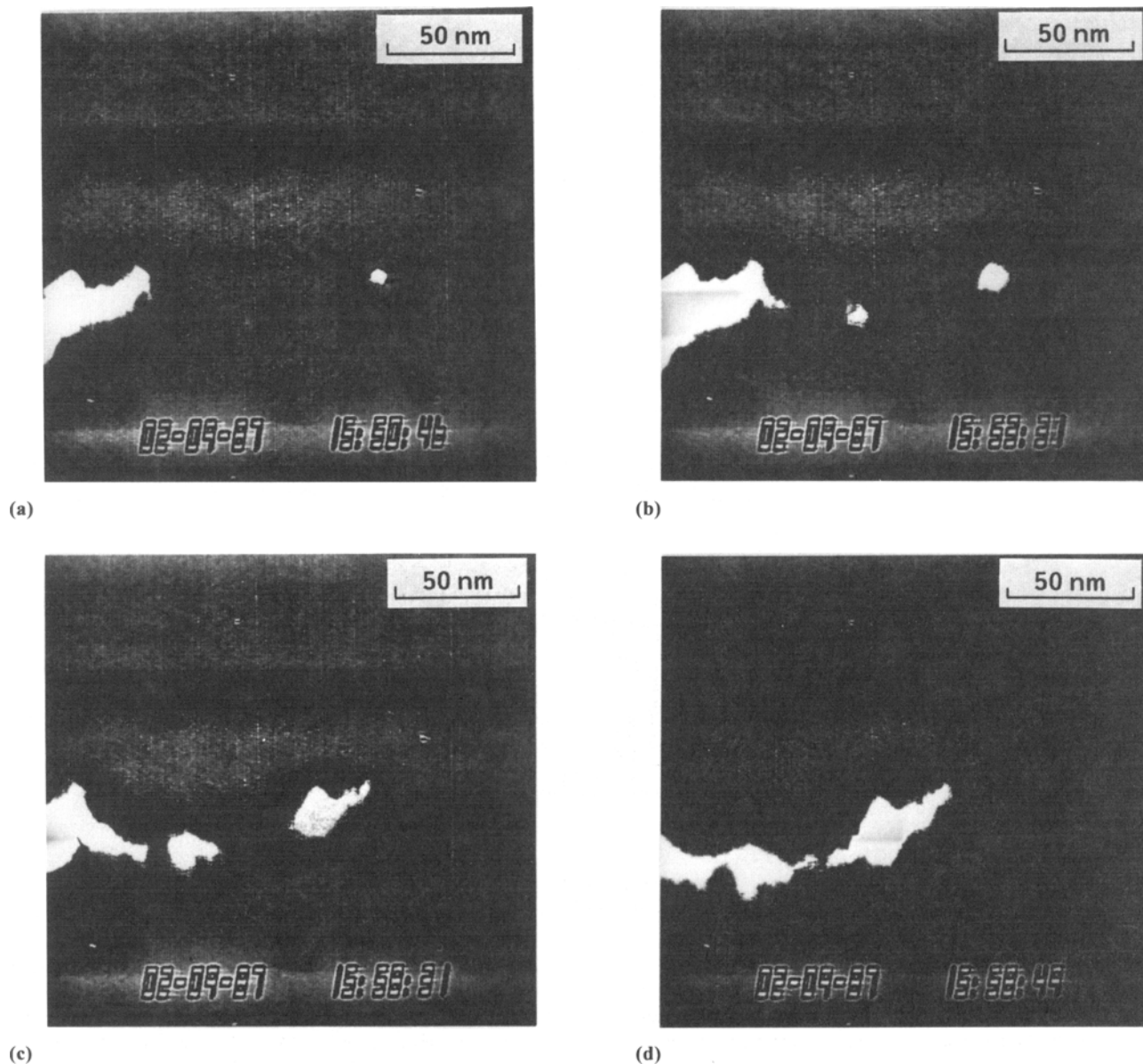


Fig. 6 Successive stages of crack growth under constant deflection in 200 torr hydrogen atmosphere showing void formation ahead of the main crack tip and coalescence into the main crack tip.

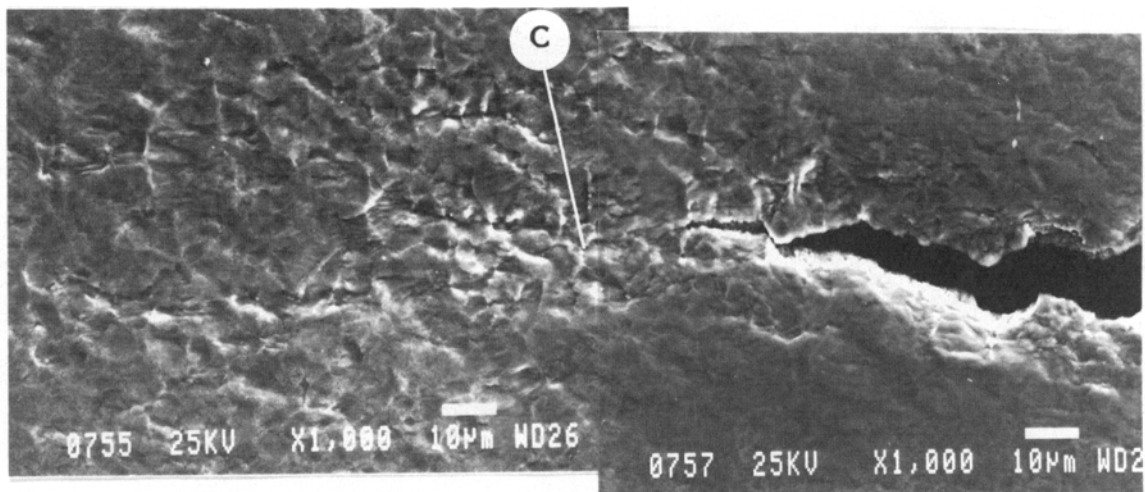
4. Conclusions

In this study, the effects of hydrogen on deformation and fracture properties of thin A533B pressure vessel steel specimens were studied, and the following conclusions were reached. Hydrogen increases the mobility and number of dislocations. Dislocations from the cell walls are released and become mobile.

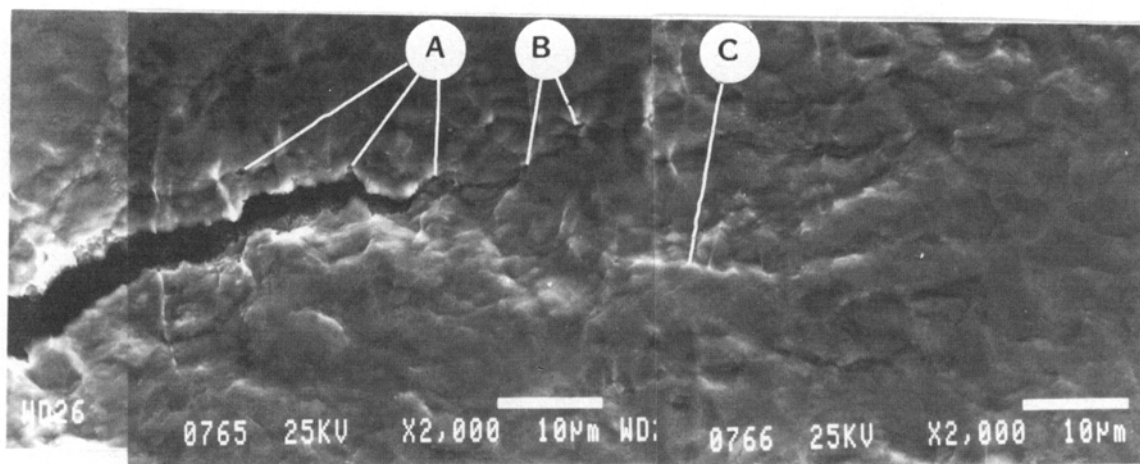
In very thin sections of the specimen, fracture takes place by a sliding-off mechanism. When thickness increases, a yielding strip plastic zone is formed ahead of the crack tip. Inside this yielding strip, the dislocations are generated, e.g., from small carbide particles, and they move into thick, dense tangled dislocation walls that form barriers on both sides of the low dislo-

cation density yielding strip. The low dislocation density yielding strip ahead of the crack tip is analogous to the Dugdale-Barenblatt model for crack growth. Due to its low dislocation density, the yielding strip is softer compared to its surroundings, and therefore, the strain at the crack tip is confined in this region, which is analogous to shear bands and PSBs.

Flow localization into a yielding strip process zone (shear band) ahead of the crack tip was observed to be an important mechanism in ductile fracture of A533B pressure vessel steel. Inside the yielding strip, hydrogen enhanced the dislocation processes, but did not change the ductile fracture mechanism. Crack tip blunting occurred by a two-corner mechanism, where a flat-nosed crack tip was formed, when the crack became dormant at the grain boundary. Further crack growth was initiated



(a)



(b)

Fig. 7 Profiles of the crack tips of the specimen shown in Fig. 1(a) at the end of the test.

by strain localization at one of the crack tip vertices. The crack propagated by void/microcrack formation ahead of the crack tip inside the yielding strip plastic zone and coalescence into the main crack tip along the slip line traces. Void nucleation ahead of the main crack tip occurred both inside the grains and at the grain boundaries, i.e., in places where the dislocation generation was probably most active, e.g., at particles inside the yielding strip. The coalescence into the main crack tip took place by a sliding off type of fracture along the shear bands producing ductile, dimpled fracture morphology.

Acknowledgments

This work was performed when one of the authors (H. Hänninen) was a visiting scientist at Materials Engineering Associates, Inc. (MEA), Lanham, Maryland, from Technical Research Centre of Finland. The funding from Electric Power Research Institute, Technical Research Centre of Finland, and Imatran Voima Foundation for the sabbatical leave is gratefully appre-

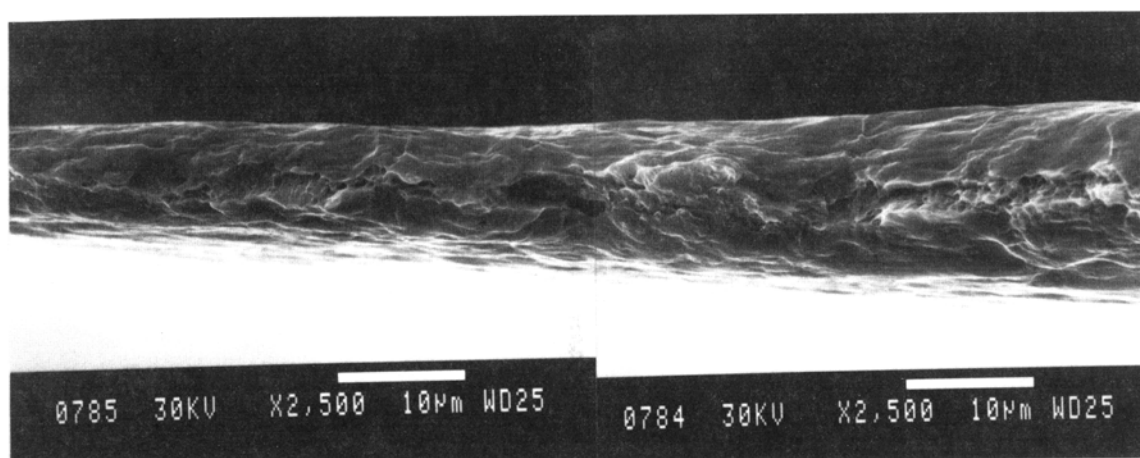
ciated. The other authors wish to acknowledge support from the Department of Energy, Division of Materials Sciences, through the Materials Research Laboratory. The authors would like to acknowledge the use of the HVEM Facility at Argonne National Laboratory and the assistance of Mr. E. Ryan.

References

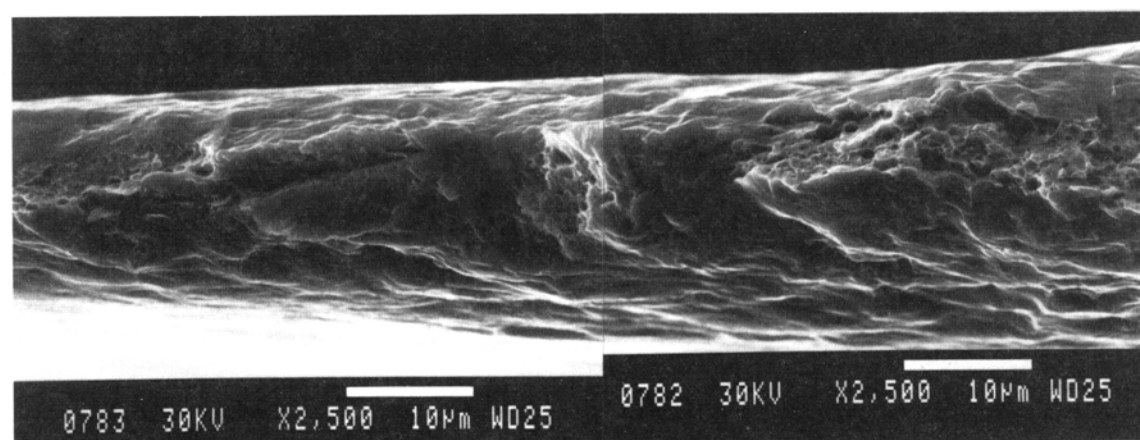
1. C.D. Beachem, *Metall. Trans. A*, Vol 3, 1972, p 437
2. C.D. Beachem, *Stress Corrosion Cracking and Hydrogen Embrittlement of Iron Base Alloys*, R.W. Staehle et al., Ed., NACE, 1977, p 376
3. J.P. Hirth, *Metall. Trans. A*, Vol 11, 1980, p 861
4. T. Tabata and H.K. Birnbaum, *Scr. Metall.*, Vol 17, 1983, p 947
5. T. Tabata and H.K. Birnbaum, *Scr. Metall.*, Vol 18, 1984, p 231
6. J. Bond, I.M. Robertson, and H.K. Birnbaum, *Scr. Metall.*, Vol 20, 1986, p 653
7. S.P. Lynch, *Advances of Mechanics and Physics of Surfaces*, Vol 2, R.M. Latanision and T.E. Fisher, Ed., 1983, p 264



(a)



(b)



(c)

Fig. 8 Fracture surfaces of one side of the crack in specimen shown in Fig. 1(a). (a) Fracture has occurred by a sliding-off mechanism. (b) and (c) Ductile, dimpled fracture is present in the middle of the specimen thickness.

8. H.K. Birnbaum, *Hydrogen Effects on Material Behavior*, N.R. Moody and A.W. Thompson, Ed., The Minerals, Metals, & Materials Society, 1990, p 639

9. H. Kimura and H. Matsui, *Scr. Metall.*, Vol 21, 1987, p 319

10. T.D. Lee, T. Goldenberg, and J.P. Hirth, *Metall. Trans. A*, Vol 10, 1979, p 199

11. O.A. Onyewuenyi and J.P. Hirth, *Metall. Trans. A*, Vol 14, 1983, p 259

12. D.S. Dugdale, *J. Mechan. Phys. Solids*, Vol 8, 1960, p 100
13. G.I. Barenblatt, *Adv. Appl. Mechan.*, Vol 7, 1962, p 55
14. G.T. Hahn and A.R. Rosenfield, *Acta Metall.*, Vol 13, 1965, p 293
15. H.-W. Liu, W. Hu, and A.S. Kuo, *Elastic-Plastic Fracture: Second Symposium, Vol II, Fracture Resistance Curves and Engineering Applications*, ASTM STP 803, C.F. Shih and J.P. Gudas, Ed., American Society for Testing and Materials, 1983, p 632
16. J.R. Rice, *Fracture—An Advanced Treatise*, Vol II, H. Liebowitz, Ed., Academic Press, 1968, p 191
17. R.L. Jones, *Proc. Int. Atomic Energy Agency Specialists' Meeting on Subcritical Crack Growth*, Vol 1, W.H. Cullen, Ed., NUREG/CP-0044, MEA-2014, 1981, p 65
18. K. Törrönen, M. Kemppainen, and H. Hänninen, EPRI Report NP-3483, Electric Power Research Institute, 1984
19. S.M. Ohr, *Scr. Metall.*, Vol 20, 1986, p 1501
20. R.J. Asaro and A. Needleman, *Scr. Metall.*, Vol 18, 1984, p 429
21. B.A. Bilby, A.H. Cottrell, and K.H. Swinden, *Proc. Royal Soc. A*, Vol 272, 1963, p 304
22. H. Mughrabi, R. Wang, K. Differt, and U. Essmann, *Fatigue Mechanisms: Advances in Quantitative Measurement of Physical Damage*, ASTM STP 811, J. Lankford et al., Ed., ASTM, 1983, p 5
23. L. Anand, *Scr. Metall.*, Vol 18, 1984, p 423